Colloid Polym Sci 275:617–626 (1997)

ORIGINAL CONTRIBUTION

D. Gregor-Svetec
S. Malej-Kveder
P. Zipper
A. Jánosi

Tensile properties and structure of polypropylene fibres spun from a blend of different polymer grades

Received: 12 December 1996
Accepted: 28 February 1997

Dr. D. Gregor-Svetec (✉) · S. Malej-Kveder
Department of Textiles
Faculty of Natural Sciences and Engineering
University of Ljubljana
Snezniska 5
1000 Ljubljana, Slovenia

P. Zipper · A. Jánosi
Institute of Physical Chemistry
University of Graz
Heinrichstraße 28
8010 Graz, Austria

Abstract The tensile behavior of fibres, spun from a blend of small percentage of plastic grade polypropylene with fibre grade polypropylene, was studied in relation to their structure. The spinning and drawing process was optimized in order to increase the elastic moduli of produced filament yarns. By such optimization of the process a tenacity of 0.7 GPa, an elastic modulus of 14.8 GPa and a dynamic modulus of 19 GPa were attained. From diffuse small-angle X-ray scattering the presence of voids, up to 11.5%, was established. Voidness of the fibrillar structure was confirmed with electron micrographs. In spite of the rather drastic changes in morphology the mechanical properties of high void fibrillar structures are good, indicating that the load bearing units of the filament have maintained their integrity. The improved mechanical behavior of highly drawn fibres spun from 10/90 plastic/fibre grade polymer blend is related to higher crystalline and above all to higher amorphous orientation.

Key words High-modulus polypropylene fibre – polymer blend – manufacturing process – X-ray diffraction – tensile properties – fibre structure

Introduction

A polyblend, sometimes called a polymer alloy, is composed of two or more polymers blended but not otherwise treated initially [1]. Many polyblends contain relatively small amounts of one of the polymers to improve the toughness or the strength, processing characteristics, wear properties, surface appearance, stiffness or flexibility, adhesiveness. The major commercial blends of isotactic polypropylene (iPP) with other polymers include addition of ethylene–propylene–diene terpolymer rubber (EPDM) to iPP to improve the low temperature impact strength, and addition of iPP to EPDM to produce thermoplastic elastomers. Blends of iPP and high-density polyethylene (HDPE) are used to improve the impact strength, to increase environmental stress-crack resistance, modulus and heat deflection temperature. In exploratory research also a wide variety of other iPP polyblends have been studied, some of them are mentioned for their practical usefulness [2].

There are only a few reports on studies of blends of different molecular weights of iPP. Deopura and Kadam [3] have found that properties of drawn iPP filaments can be improved by blending a fibre-grade polymer with a high molecular weight polymer (HMPP). Results by Bet et al. [4] support these findings. They obtained the highest value of elastic modulus (8.4 GPa) for a two-stage drawn fibre, spun from a blend of fibre-grade PP with 3% of HMPP. Mahajan et al. [5] achieved the optimum breaking stress (0.74 GPa) and modulus (7.34 GPa) of the drawn samples at about 6% HMPP blend composition and inferior tensile strength and modulus at a higher percentage

of the second component. Geleji et al. [6] reported improvement of mechanical properties of the drawn fibres upon increasing the amount of HMPP in the blend. The highest tensile strength of 0.43 GPa and elastic modulus of 5 GPa were given by a 75% HMPP blend sample drawn at 130 °C with draw ratio of 5.

As part of a larger systematic study of the role of various spinning and drawing conditions and of ways to optimize the fabrication processes in order to achieve a high value of the elastic modulus of drawn filaments, we investigated the tensile properties and structure of a range of laboratory manufactured PP multifilament yarns. In our work, we undertook study on yarns, produced from the blend of a fibre-grade PP polymer with a plastic-grade PP polymer in the composition range of 10–50 wt% HMPP content. In the present paper the tensile properties and structure of PP yarns with the greatest value of elastic modulus obtained, are presented.

Experimental

Preparation of PP multifilament yarns

Filaments were spun from a blend of two commercial Hoechst polypropylene chips, Hostalen PPU 1780F2, a fibre grade homopolymer with MFR = 18 g/10 min and Hostalen PPN 1060F, a plastic grade homopolymer with MFR = 2 g/10 min. (*The melt flow rate (MFR) was determined as the amount of polymer extruded at the temperature of* 230 °C *with the forcing load of* 2160 g *in* 10 min.) Hostalen PPU 1780F2 with $\overline{M}_w$ = 210.000 g/mol is a narrow molecular weight distribution polymer, the so-called controlled rheology or CR-polymer, with the ratio of molecular weight to number average molecular weight ($\overline{M}_w/\overline{M}_n$) of 3.3, while Hostalen PPN 1060F with $\overline{M}_w$ = 280.000 g/mol is a broad molecular weight distribution polymer, with $\overline{M}_w/\overline{M}_n$ = 5. The blend composed of 90/10 fibre/plastic grade polymer by weight was mixed manually. The melt spinning and in-line drawing of PP multifilament yarn was carried out on an Extrusion Systems Ltd. laboratory spin-draw device. From the preceding experiments [7] the optimal process path variables were established in order to achieve maximal elastic modulus of the multifilament yarns produced. The filaments were extruded at a rate of 21.7 g/min through a spinneret with ten holes of diameter 0.35 mm each. The temperature of the melt at the spinneret was 245 °C. Cooling of the resultant filaments was achieved with cross-flow air quenching at the temperature of 6 °C. The as-spun filaments were three-stage drawn at 50 °C, with overall draw ratio of 15.25, in a continuous spin-drawing process. Moderately, continuously drawn multifilament yarn was additionally drawn to the limiting draw ratio on a Zimmer laboratory draw device. In this subsequent slower stage the yarn was drawn through a hot-plate at 130 °C with draw ratio of 2.52, and at 145 °C with draw ratio of 2.92. No separate heat setting step was carried out.

Tensile testing

The tensile properties of the PP multifilament yarns were measured with an Instron 6022 tensile testing machine. Samples of initial gauge length of 25 cm were stretched at a crosshead speed of 1.6 mm/s for discontinuously highly drawn yarns and of 5.5 mm/s for continuously moderately drawn yarn. Conventional stress–strain data were obtained under conditions of controlled temperature and humidity (T = 21°, relative humidity = 65%). Mechanical data presented in this article are the average of 50 parallels and stress–strain curves of about 20 parallels.

Structural characterization

Wide-angle X-ray scattering (WAXS) and small-angle X-ray scattering (SAXS) techniques were used to explore the structure of PP multifilament yarns. Copper radiation (CuK_α λ = 0.154 nm) was monochromatized by means of a 10 μm Ni filter. WAXS and SAXS film patterns were taken on a vacuum flat-film camera with pinhole collimation. WAXS curves (*intensity as a function of scattering angle* (2θ)) were made for normal transmission geometry of samples by using a two-circle goniometer developed by Kratky. SAXS curves were obtained by using a Kratky block-camera with slit collimation. Scattered intensities were registered with a position sensitive detector Braun PSD 50M or with a conventional proportional detector.

The degree of crystallinity was estimated by the Hermans and Weidinger method [8] over the angular range from 2θ = 10° to 30°. The crystallinity was calculated as the ratio of the integrated scattering under the resolved crystalline peaks to the total scattering of the sample.

Apparent crystallite dimensions were determined, by means of Scherrer's equation [9], from the half-widths of diffraction curves of crystalline peaks which were approximated by pseudo-Voigt functions:

$$L_{hkl} = \frac{K\lambda}{\beta_0 \cos\theta}, \quad (1)$$

where L_{hkl} is the mean size of the crystallites perpendicular to the planes (hkl), β_0 is the breadth of the reflection profile (in radians) at half-maximum intensity, and K is a constant that is assigned a value of 0.9 for PP.

The crystalline orientation function [Eq. (2)] was calculated with the help of (1 1 0) and (0 4 0) reflections, using the Wilchinsky relation [10] for a monoclinic crystal system [Eq. (3)]. In monoclinic PP crystallites the macromolecules are helices whose axes lie along the c-crystallographic axis in the direction of the fibre axis. Orientation of the crystallite axis c with respect to the reference direction Z (the fibre axis) is given by

$$f_{cry} = f_{c,Z} = \tfrac{1}{2}(3\langle\cos^2\phi_{c,Z}\rangle - 1)\,, \tag{2}$$

where $\langle\cos^2\phi_{c,Z}\rangle$ is the mean-square cosine (averaged over all the crystallites) of the angle between the fibre axis and the c-crystallographic axis and was calculated from

$$\langle\cos^2\phi_{c,Z}\rangle = 1 - 1.099\langle\cos^2\phi_{110,Z}\rangle - 0.901\langle\cos^2\phi_{040,Z}\rangle\,. \tag{3}$$

The long period was determined from the meridional SAXS reflection via the calculated one-dimensional intensity function $I_1(h)$, with the scattering vector h defined as

$$h = \frac{4\pi}{\lambda}\sin\theta\,. \tag{4}$$

The experimental scattering function, measured with the fibre axis perpendicular to the line-shaped primary beam, was assumed to be proportional to $I_1(h)$ and was approximated with the following expression based on a stacking model as described by Brämer [11, 12]

$$I_1(h) \propto \frac{1}{h^2}\,\mathrm{Re}\left[\frac{(1-F_c)(1-F_a)}{1-F_D}\right]. \tag{5}$$

Here $F_c = \mathrm{FT}(P_c)$, $F_a = \mathrm{FT}(P_a)$, and F_D is the convolution of both functions $F_D = F_c * F_a$. The functions $P_c(x_c)$ and $P_a(x_a)$ describe the distributions of the thickness of the crystalline and amorphous layers, respectively, and can be modeled with Gaussian or asymmetrical functions (exponentials, Reinhold's distribution [13]).

From diffuse small-angle X-ray scattering (measured with the fibre axis aligned parallel to the streak of the primary beam) the volume fraction of voids present in the solid polymers was estimated. SAXS curves were evaluated in accordance with Porod's theory, by assuming a dense two-phase system (polymer/voids) [14, 15]. For a two-phase system with known electron density difference $(\Delta\rho)_{1,2}$ between the two phases, the volume fractions w_1 and $w_2 = 1 - w_1$ of the two phases follow from

$$\overline{(\Delta\rho)^2} = w_1 \cdot w_2 (\Delta\rho)^2_{1,2}\,, \tag{6}$$

where $\overline{(\Delta\rho)^2}$ is the mean square fluctuation of electron density.

The correlation length (l_c) is a mean value of the extension of a coherently scattering domain and was obtained as the quotient of the first and second moments of the experimental SAXS curve.

The crystalline fraction in fibres was evaluated also from density data and DSC-thermograms. The density of PP multifilament yarns was determined with the flotation method as described by Juilfs [16], using a mixture of isopropylalcohol and water. The crystallinities of the samples were then calculated by the equation

$$x_{\mathrm{DENSITY}} = \frac{\rho_c(\rho - \rho_{am})}{\rho(\rho_c - \rho_{am})}\cdot 100\%\,, \tag{7}$$

where ρ is the sample density and ρ_c and ρ_{am} are the densities of the crystalline and amorphous phases, respectively.

DSC-thermograms were recorded from 40 °C to 200 °C, with a heating rate of 10 °C/min, on a DSC-7 Perkin-Elmer apparatus. From the measured heat of fusion (ΔH) the crystallinity was derived from the following equation

$$x_{\mathrm{DSC}} = \frac{\Delta H}{\Delta H_c}\cdot 100\%\,, \tag{8}$$

where ΔH_c is the heat of fusion of 100% crystalline PP and was assumed in this work as 209 J/g.

The average molecular orientation and dynamic modulus were obtained by the sonic-velocity method. The velocity of sound waves in the filament was measured on a Morgan's Dynamic Modulus Tester PPM-5R. Relations between sonic velocity (c), dynamic modulus (E_{dy}) and the molecular orientation are defined by

$$E_{dy} = \rho c^2\,, \tag{9}$$

$$f_{or} = \frac{1 - (c^2_{un}/c^2)}{1 - (c^2_{un}/c^2_{id})}\,, \tag{10}$$

where f_{or} is the average orientation function, c_{un} is the sonic velocity of the unoriented sample and c_{id} is the sonic velocity of the perfectly oriented sample.

The amorphous orientation function (f_{amo}) was calculated from the experimental value of the dynamic modulus (E_{dy}), the fraction of the crystalline phase (x_{WAXS}) and the crystalline orientation function (f_{cry}) determined by WAXS measurements in a manner applied to PP by Samuels [17]

$$\frac{3}{2}(\Delta E^{-1}) = \frac{x_{\mathrm{WAXS}} f_{cry}}{E^0_{t,cry}} + \frac{(1 - x_{\mathrm{WAXS}}) f_{amo}}{E^0_{t,amo}}\,,$$

$$(\Delta E^{-1}) = E^{-1}_{un} - E^{-1}_{dy}\,, \tag{11}$$

Colloid & Polymer Science, Vol. 275, No. 7 (1997)

where E_{un} is the sonic modulus of the isotropic phase, $E^0_{t,cry}$ and $E^0_{t,amo}$ are the transverse moduli of completely oriented crystalline and amorphous phases, respectively. Morphological studies involved scanning electron microscopy of the filament surface. A JEOL JSM-2 electron microscope was used for all morphological studies. Several samples were split to expose the interior structure. Filaments were also etched in a chromic acid solution at room temperature. Magnification is indicated by a 10 μm bar on the micrographs.

Results and discussion

Tensile properties

The tensile properties of PP filaments are strongly influenced by their physical structure which is controlled by the choice of the starting material and the fibre formation conditions. By optimized slow multi-stage drawing of filaments spun from a blend with prevailing polymer of narrow molecular weight distribution, known for its good spinnability and drawability, a high overall draw ratio could be reached. Highly drawn PP filaments, stretched to the maximum attainable draw ratio in a two-step drawing process, have reached excellent mechanical properties. Linear density and tensile properties are given in Table 1 and the stress–strain curves of drawn PP multifilament yarns are shown in Fig. 1.

In the case of a particulate-filled or two-phase composite system, the resultant modulus of the composite is a function of the moduli of the individual pure components, the volume of the weight fraction, the geometry and packing of the disperse phase, and the Poisson ratio of the matrix. Four possible ways to determine the dependence of modulus on composition are "the rule of mixture" for the Voigt model, "the rule of mixture" by the Reuss equation, Nielsen and Halpin modified Kerner equation and the simplex equation [18]. The modulus of polymer blends can be expressed by the Kleiner's simplex equation [19] where the empirical parameter β_{12} is obtained from Eq. (13).

$$E = W_1E_1 + W_2E_2 + \beta_{12}W_1W_2\,, \tag{12}$$

$$\beta_{12} = 4E_{12} - 2E_1 - 2E_2\,, \tag{13}$$

E is the modulus of the blend, E_1 and E_2 are the moduli of pure components, W_1 and W_2 are the corresponding weight fractions and E_{12} represents the modulus of the 50/50 blend. Positive and negative values of β_{12} represent nonlinear synergism and antagonism, respectively. In the case of all three samples the calculated values of β_{12} were positive indicating a synergistic effect of blending on modulus. The largest positive deviation from the additivity rule is shown by the multifilament yarn discontinuously highly drawn at 145 °C. This yarn reached an E_0 value as high as 14.8 GPa. Dynamic moduli obtained from sound velocity measurements also exhibit very high values for highly drawn yarns, and a positive deviation from predicted values.

Discontinuously highly drawn multifilament yarns exhibit, besides high moduli, high values of specific stress at break, which is a measure of the resistance to steady forces. The specific work of rupture, sometimes called the toughness and defined as the energy needed to break a fibre, gives a measure of the ability of the material to withstand sudden shocks of given energy. Low toughness, together with low breaking extension, high tenacity and moduli of highly drawn yarns implies that after the initial high resistance to stretching a brittle breakage will occur. Continuously moderately drawn multifilament yarn of low tenacity and higher toughness is easily extensible. The

Table 1 Linear density and mechanical properties of continuously moderately and of discontinuously highly drawn PP multifilament yarns

Sample	T_t (tex)	σ_{br} (GPa)	ε_{br} (%)	A_{br} (kJ/kg)	E_0 (GPa)	$E_{0,pr}$ (GPa)	E_{dy} (GPa)	$E_{dy,pr}$ (GPa)
Continuously drawn at 50 °C	51.96	0.31	79.53	209.8	2.68	2.37	9.69	9.22
Discontinuously drawn at 130 °C	22.95	0.68	11.15	47.35	12.00	11.86	17.00	15.70
Discontinuously drawn at 145 °C	19.69	0.70	9.00	44.70	14.80	13.52	19.00	18.40

T_t linear density – weight per unit length; tex is the weight in grammes of one kilometer.
σ_{br} specific stress and break – rupture load divided by the original weight per unit length.
ε_{br} extension at break – change in length divided by the initial length.
A_{br} specific work of rupture – area under the curve of specific stress against strain divided by the weight per unit length and by the initial length.
E_0 elastic modulus – tangent of the angle between the initial part of the curve and the horizontal axis.
$E_{0,pr}$ predicted elastic modulus for a blend – E calculated from the simplex equation [Eq. (12)].
E_{dy} dynamic modulus – product of a velocity of sound waves and density.
$E_{dy,pr}$ predicted dynamic modulus for a blend – E calculated from the simplex equation [Eq. (12)].

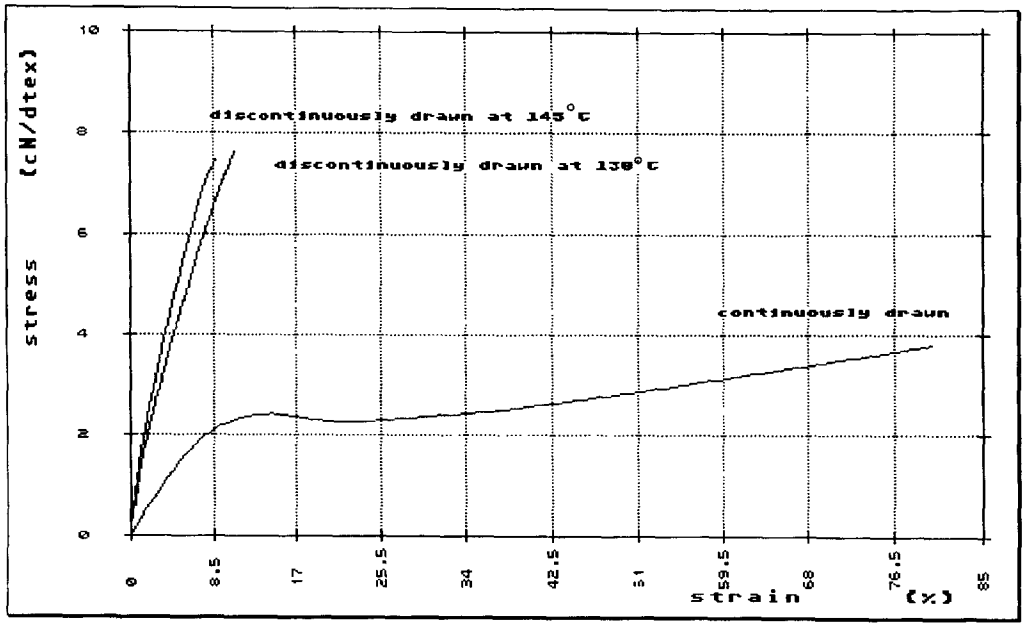

Fig. 1 Stress–strain curves of continuously moderately and of discontinuously highly drawn PP multifilament yarns

shape of the stress–strain curve (Fig. 1) shows after an initial linear portion a marked yield point, and up to the break, a region of low slope, where large extensions are produced by small increases in stress. Both discontinuously highly drawn multifilament yarns exhibit brittle mode of deformation behavior, with short initial period of steep slope, no apparent yield point, and a regime of sharply rising stress until fracturing occurred at extension of 11% for the yarn drawn at 130 °C and 9% for yarn drawn at 145 °C.

Morphological and structural characterization of PP multifilament yarns

Isotactic PP is a polymorphic material and is capable of crystallizing in three different crystalline modifications and a mesomorphic, so-called smectic form [20]. WAXS film patterns of drawn multifilament yarns, taken in order to determine the crystalline modifications present, are shown in Figs. 2–4, together with WAXS two-dimensional intensity maps.

Continuously moderately drawn multifilament yarn shows wide equatorial spots of the (1 1 0), (0 4 0) and (1 3 0) planes united in one reflection on the WAXS film pattern (Fig. 2A). The presence of oriented so-called "smectic" structure in this sample was confirmed by WAXS intensity maps (Fig. 2B). Overlapping reflections of (1 1 0), (0 4 0) and (1 3 0) planes are united in one equatorial peak at $2\theta = 14.6°$, whereas a second broad peak exists at $2\theta = 21.2°$. In this partially ordered phase of iPP the individual chains maintain the threefold helical conformation and the chains are parallel. The packing of the chains perpendicularly to their axis is more disordered than along the axes, though the relative displacements and orientations of neighboring chains are not completely random. Gailey and Ralston [21] and Gezovich et al. [22] suggested the possibility that this less ordered form of iPP is composed of small crystallites of hexagonal form, whereas Bodor et al. [23] and Farrow [24] assumed crystallites of monoclinic form. It was also suggested [20] that the rather diffuse X-ray diffraction pattern is associated with the occurrence of paracrystallinity. In our opinion, the α-iPP or monoclinic form is present in continuously moderately drawn multifilament yarn and the overlapping of equatorial reflections is the consequence of the broadening effect of very small or very imperfect crystallites.

The small value (3.4 nm) of the lateral crystallite dimensions as determined from the half-width of the equatorial peak confirms the presence of small crystallites. Even if we were able to separate all three united equatorial reflections, their intensities would be small, the values of half-width of peaks would be large, and so the crystallite size would remain small. This implies that crystal size broadening may be considered to be responsible for the typical WAXS pattern, as also interpreted by Bodor et al. [23].

Both highly discontinuously drawn multifilament yarns show discrete reflections of α-iPP crystal structure on the WAXS film pattern (Figs. 3A and 4A). This typical pattern of a well-oriented fibrous structure, with the above broad equatorial maximum split up into narrower (1 1 0), (0 4 0) and (1 3 0) reflections is clearly seen on the WAXS

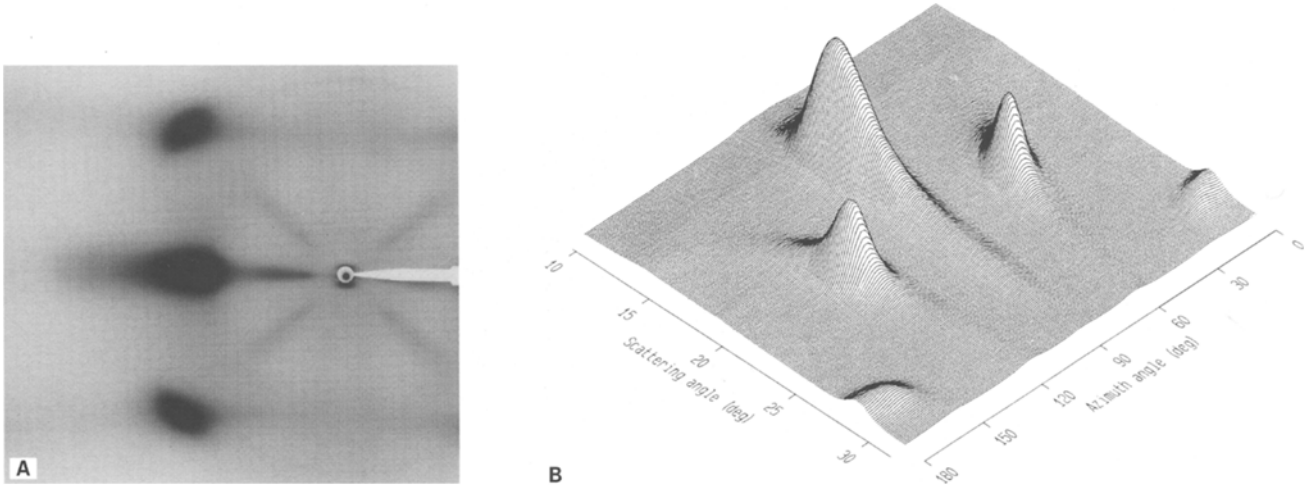

Fig. 2A WAXS film pattern (fibre axis vertical) and **B** WAXS intensity maps of continuously moderately drawn PP multifilament yarn

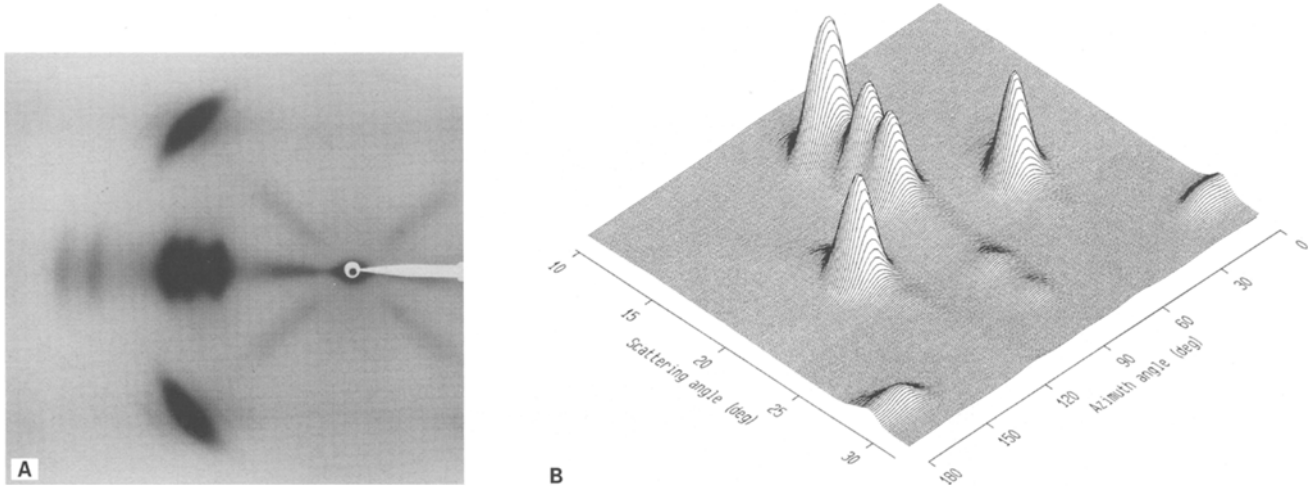

Fig. 3A WAXS film pattern (fibre axis vertical) and **B** WAXS intensity maps of PP multifilament yarn discontinuously highly drawn at 130 °C

intensity maps too (Figs. 3B and 4B). Only *c*-axis orientation of monoclinic crystallites is present in these two yarns.

SAXS film patterns of drawn PP multifilament yarns, together with the measured SAXS curve approximated with the calculated model function, are shown in Figs. 5 and 6. The measured SAXS curve of the oriented fibre is interpreted as a cross-section function. By dividing it with the squared value of the scattering vector a fictive scattering curve is calculated and then approximated with the model function. The model curves were calculated within a larger range of the scattering vector as was taken for the analysis of the scattering curves; therefore, the deviation of the experimental function from the calculated one at small values of the scattering vector appeared. (*The long period was determined in the range between* 0.03 $Å^{-1}$ *and* 0.18 $Å^{-1}$ *for continuously moderately drawn yarn and between* 0.02 $Å^{-1}$ *and* 0.18 $Å^{-1}$ *for discontinuously highly drawn yarn.*) Continuously moderately drawn yarn exhibits a two-point pattern with weak intensity maxima on the meridian, corresponding to a long period of 11.5 nm and a weak diffuse equatorial scattering (Fig. 5A) which indicates the presence of microvoids. As seen on the SAXS film pattern of discontinuously highly drawn yarn no discrete meridional small angle reflection appeared (Fig. 6A).

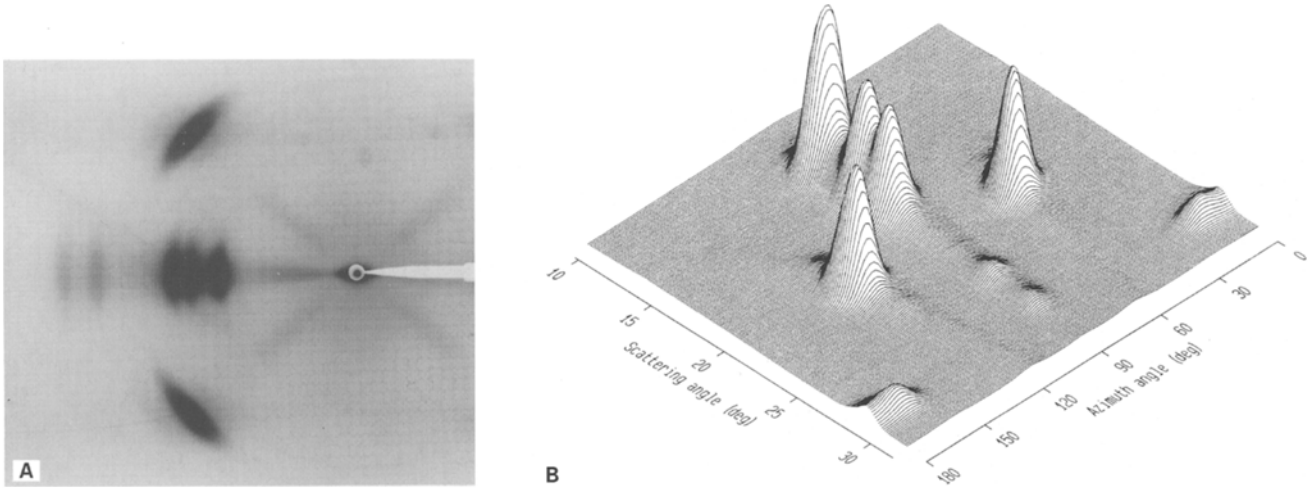

Fig. 4A WAXS film pattern (fibre axis vertical) and **B** WAXS intensity maps of PP multifilament yarn discontinuously highly drawn at 145 °C

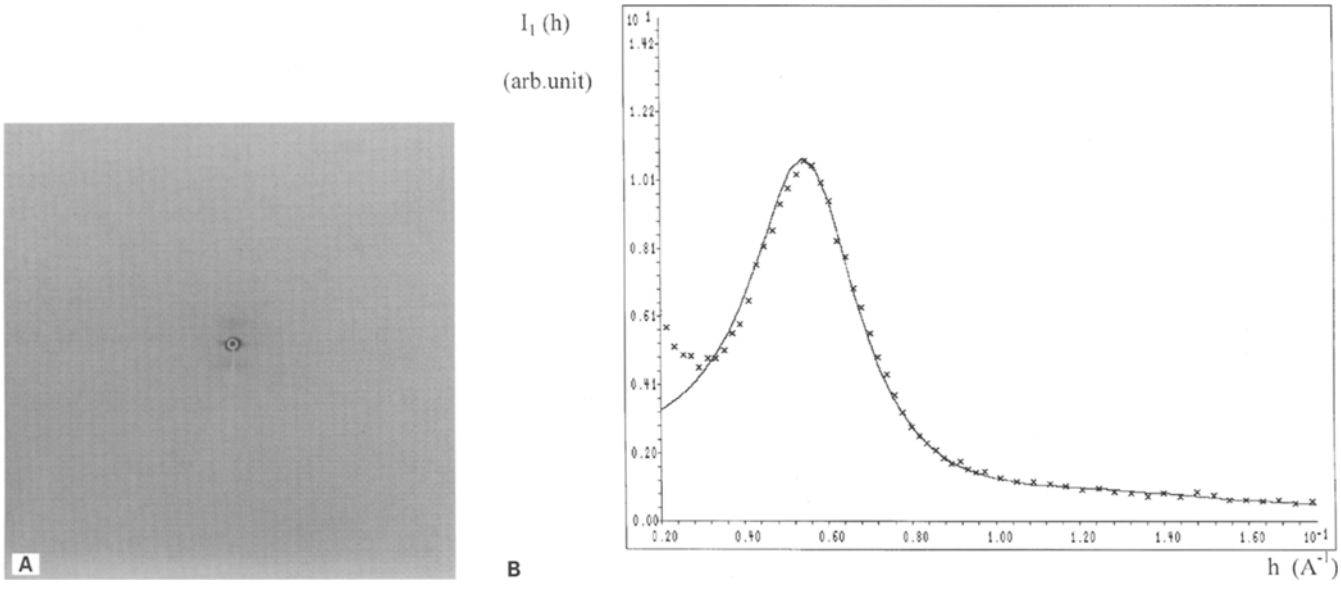

Fig. 5A SAXS film pattern (fibre axis vertical) and **B** measured meridional SAXS curve of continuously moderately drawn PP multifilament yarn (xxxx) approximated with the model function (——)

The absence of the meridional reflection could be explained by a dissolution of lamellar structure, assuming that the regular alternation of crystalline and amorphous regions is disrupted on drawing by extension of the molecular chains and subsequent formation of voids. These crystalline and amorphous regions are now irregularly rearranged in adjacent microfibrils. As a result, there is a lack of sufficient scattering power, the difference in electron density decreases considerably, which diminishes the intensity of the meridional reflection. At the same time, very strong diffuse equatorial scattering appears, due to inhomogenities in electron distribution. A typical "diamond" shaped pattern indicates the presence of large voids elongated parallel to the filament axis.

The apparent crystallite size and long period of drawn PP multifilament yarns are presented in Table 2. As mentioned previously, the apparent crystallite size of continuously moderately drawn yarn is low, as well as the long

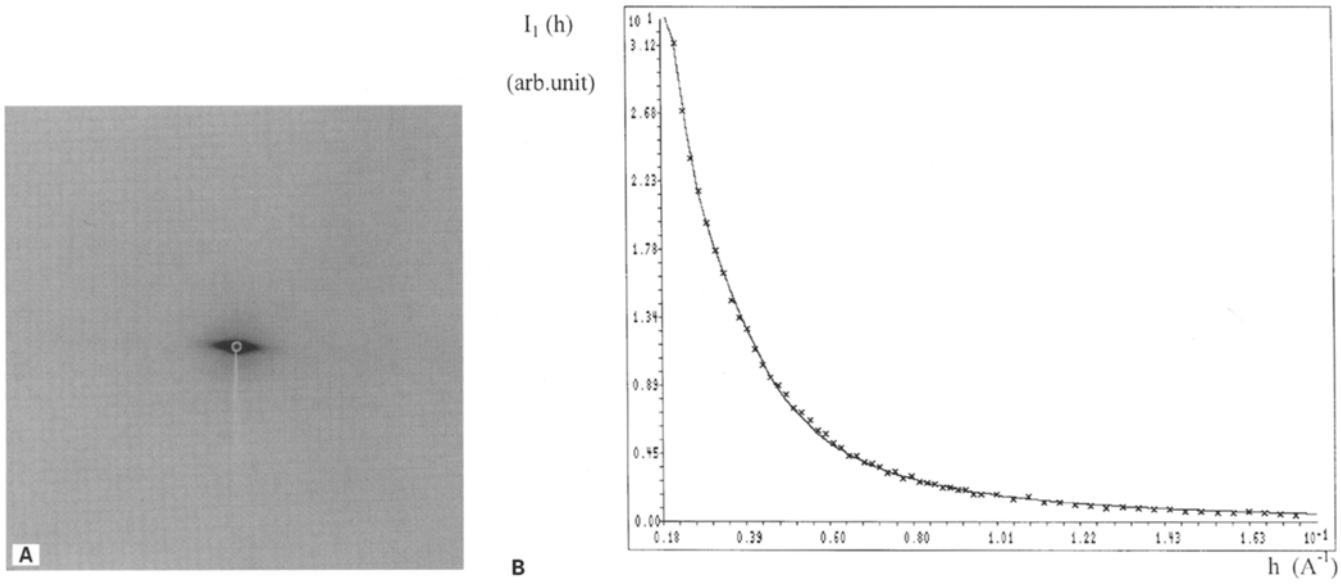

Fig. 6 **A** SAXS film pattern (fibre axis vertical) and **B)** measured meridional SAXS curve of PP multifilament yarn discontinuously highly drawn at 145 °C (xxxx) approximated with the model function (——)

Table 2 Apparent crystallite size in the direction perpendicular to the planes (1 1 0), (0 4 0), (1 3 0) (marked L_{110}, L_{040}, L_{130}) and to the planes (1 1 1), (0 4 1), ($\bar{1}$ 3 1) united in one peak (marked L_{hkl}) and long period (L) of continuously moderately and discontinuously highly drawn PP multifilament yarns

Sample	L_{110} (nm)	L_{040} (nm)	L_{130} (nm)	L_{hkl} (nm)	L (nm)
Continuously drawn at 50 °C		3.4*		5.0	11.5
Discontinuously drawn at 130 °C	8.2	9.4	7.6	7.0	22.9
Discontinuously drawn at 145 °C	8.9	9.5	8.0	7.1	29.6

* Determined from the equatorial reflections (1 1 0), (0 4 0) and (1 3 0) united in one peak.

period. With additional hot drawing the size of crystallites and the long period increases. The high values for the long periods, e.g, about 30 nm for yarn highly drawn at 145 °C, are only approximately predicted values, because of the absence of discrete reflections, and were obtained from the constructed model function.

In order to obtain information about the average size and concentration of the microvoids the correlation length l_c and the volume fraction of microvoids w_1 were determined from the SAXS curves. For continuously moderately drawn PP multifilament yarn the values obtained for the correlation length $l_c = 25$ nm and for the volume fraction of microvoids, $w_1 = 1.7\%$, are in the range of values reported for polymers. Much higher values of microvoid content and size were obtained for discontinuously highly drawn multifilament yarns. A value of $l_c = 41.3$ nm and $w_1 = 10.5\%$ was found for yarns drawn at 130 °C and $l_c = 40.5$ nm and $w_1 = 11.5\%$ for yarn drawn at 145 °C.

Electron microscopy was used to examine in some detail the morphological changes which occurred on drawing. In Fig. 7 surface features of moderately and highly drawn filaments are shown. Continuously moderately drawn PP multifilament yarn remained transparent after drawing. Under the microscope, filaments exhibited a smooth surface, without any surface features (Fig. 7A). Discontinuously highly drawn yarns became visibly opaque after drawing. This "whitening" phenomenon indicates the presence of great many voids with magnitude of the order of optical wave length. Investigation of the surface by electron microscopy revealed craze-like markings perpendicular to the filament axis (Fig. 7B). A craze can be defined as a zone spanned by aligned fibrils alternating with elongated void both being parallel to the draw axis [25]. These planes correspond to the strain-induced "transverse lines" observed by optical microscopy. The birefringence of these filaments could not be measured exactly, because of the many transverse lines present.

Examination of the internal texture by splitting and etching indicated that morphological changes were not restricted only to surface layers. While continuously moderately drawn filaments could not be split without extensive plastic deformation, discontinuously highly drawn filaments could be split, because of low lateral cohesion of

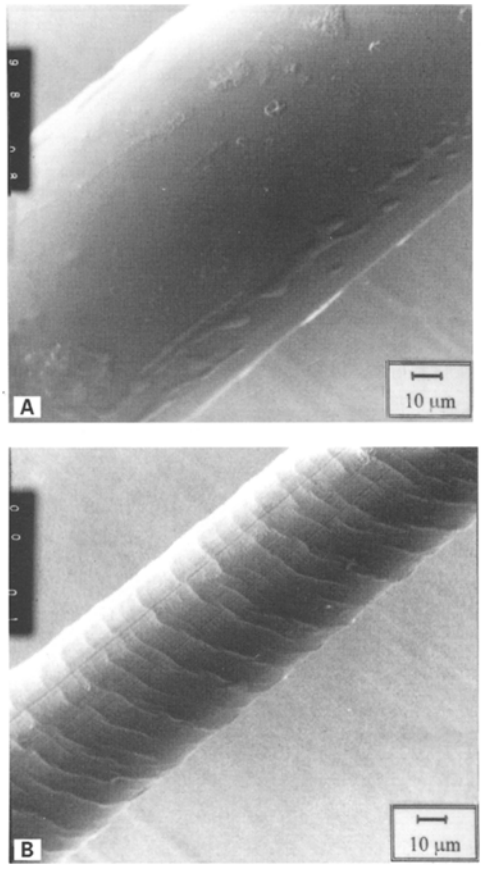

Fig. 7 Electron micrographs of surface **A** of continuously moderately drawn PP multifilament yarn and **B** of PP multifilament yarn discontinuously highly drawn at 145 °C

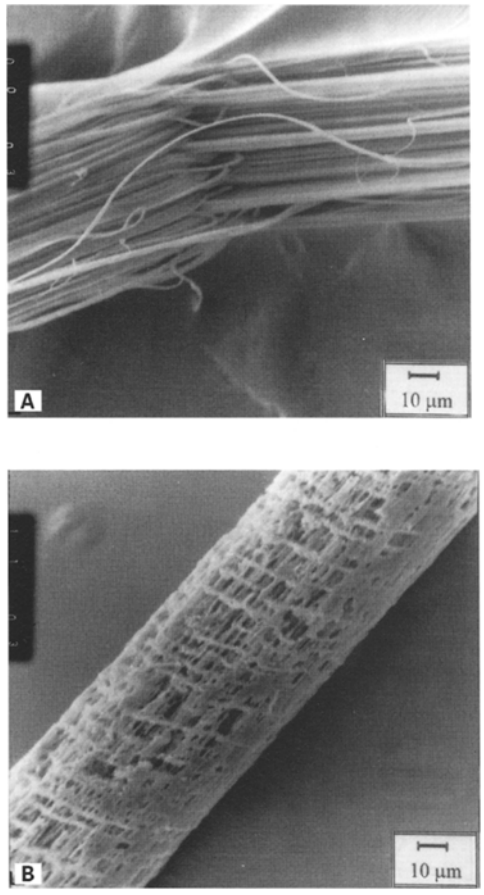

Fig. 8 Electron micrographs of the internal structure of PP multifilament yarn discontinuously highly drawn at 145 °C revealed by **A** splitting and **B** chromic acid etching

the highly developed fibrillar structure seen in Fig. 8A. After 100 h chromic acid etching at room temperature, a bulk of the filament was etched, because of its highly voided structure, and only small platelets of acid resistant structure remained (Fig. 8B).

The quantitative data summarized in Table 3 clearly show that differences exist between the structural characteristics of the continuously moderately and the discontinuously highly drawn PP multifilament yarns, i.e., crystallinity and molecular orientation were increased by further drawing. The degree of crystallinity, evaluated from WAXS curves and DSC-thermograms exhibits the same tendency of increasing with increasing draw ratio. On the other hand, the crystallinity calculated from density data does not show the same increasing tendency, because the distribution of microvoids throughout the polymer matrix decreases the density of the discontinuously highly drawn yarns, especially for yarn drawn at 130 °C.

Table 3 Degree of crystallinity evaluated from WAXS curves (x_{WAXS}), DSC thermograms (x_{DSC}) and density data ($x_{DENSITY}$), average molecular orientation (f_{or}), crystalline orientation (f_{cry}) and amorphous orientation (f_{amo}) of continuously moderately and discontinuously highly drawn PP multifilament yarns

Sample	x_{WAXS} (%)	x_{DSC} (%)	$x_{DENSITY}$ (%)	f_{or}	f_{cry}	f_{amo}
Continuously drawn at 50 °C	25.5	43.9	40.5	0.778	0.856	0.591
Discontinuously drawn at 130 °C	38.5	52.6	16.8	0.883	0.906	0.773
Discontinuously drawn at 145 °C	43.5	54.1	42.0	0.895	0.913	0.836

The highest degree of crystallinity was reached with yarn discontinuously highly drawn at 145 °C. A value of 54% was determined from DSC-measurement. This yarn also exhibits the highest molecular orientation (Table 3). The average orientation function, as well as the crystalline and amorphous orientation function increased with further drawing of the PP multifilament yarn. The orientation function of the crystallite axis c increased in highly drawn yarns in comparison to the continuously moderately drawn yarn, and leveled off at high draw ratios, i.e., the difference between both highly drawn yarns is in the range of the value's statistical deviation. The orientation function of amorphous chains behaves differently, its value increases with the draw ratio. A high value of elastic moduli is therefore associated mainly with the orientation function of amorphous chains at high draw ratio.

Conclusions

High tenacity melt-spun PP multifilament yarns, with an elastic modulus of 14.8 GPa and dynamic modulus of 19 GPa could be produced in a multi-stage drawing process, using industrially feasible conditions. Excellent mechanical properties were attained with rapid cooling of extruded filaments, immediate three-stage drawing at 50 °C in a continuous spin-drawing process, which was followed by a slower discontinuous hot drawing at evidently the most suitable temperature of 145 °C. By blending a CR-polymer of sufficiently low molecular weight with a small percentage of high molecular weight polymer, maximization of elastic modulus at the given process conditions was achieved. The positive deviation reflected by the 90/10 fibre/plastic grade polymer from the values predicted by the Kleiner's simplex equation, suggests good compatibility of PP polymers of different molecular weight.

PP multifilament yarn produced in a continuous spin-drawing process has an oriented "smectic" structure whereas discontinuously highly drawn yarns show a highly oriented fibrillar structure with only c-axis oriented monoclinic crystalline modification present. In highly strained yarns, localized fibrillation resulted in the formation of many elongated voids and a craze-like structure is produced. The mechanical properties of highly voided fibrillar structure are good, indicating that in spite of the rather drastic changes in morphology the load bearing units of the filament have maintained their integrity. The improved mechanical behavior of these highly drawn yarns is related mainly to higher amorphous orientation and to an increase in the fraction of taut tie molecules, i.e., extended molecules which are bridging the amorphous layers and connecting the crystalline layers in microfibrils and between them.

References

1. Markin C, Williams HL (1980) J Appl Polym Sci 25:2451–2466
2. Deanin RD, Chuang C (1993) In: Vasile C, Seymour RB (eds) Handbook of Polyolefins: Synthesis and Properties, pp 791–793. Marcel Dekker, New York
3. Deopura BL, Kadam S (1986) J Appl Polym Sci 31:2145–2155
4. Bet DG, Srivastava VK, Mani BP, Deopura BL (1986) 43. All India Conf, The Textile Association India, Bombay, December, pp 276–280
5. Mahajan SJ, Bhaumik K, Deopura BL (1991) J Appl Polym Sci 43:49–56
6. Geleji F, Kóczy L, Fülöp I, Bodor G (1977) J Polym Sci: Polym Symp 58: 253–273
7. Gregor D (1990) Thesis presented for the Master of Science Degree, University in Ljubljana, pp 33–46
8. Weidinger A, Hermans PH (1961) Makromol Chem 50:98–115
9. Klug HP, Alexander LE (1973) X-ray Diffraction Procedures, p 687. Wiley, New York
10. Wilchinsky ZW (1960) J Appl Phys 31:1969–1972
11. Wenig W, Brämer R (1978) Colloid Polym Sci 256:125–132
12. Brämer R (1974) Colloid Polym Sci 252:504–515
13. Reinhold G, Fischer EW, Peterlin A (1964) J Appl Phys 35:71–74
14. Porod G (1982) In: Glatter O, Kratky O (eds) Small Angle X-ray Scattering, pp 18–50. Academic Press, London
15. Jánosi A (1986) Z Phys B Condensed Matter 63:375–381
16. Juilfs J (1959) Melliand Textilberichte 40:963–966
17. Samuels RJ (1974) Structured Polymer Properties, pp 41–51. Wiley, New York
18. Teh JW (1983) J Appl Polym Sci 28:605–618
19. Lee YK, Jeong YT, Kim KC, Jeong HM, Kim BK (1991) Polym Engn Sci 31: 944–953
20. Brückner S, Meille SV, Petraccone V, Pirozzi B (1991) Prog Polym Sci 16:361–404
21. Gailey JA, Ralston PH (1964) Soc Plastics Eng Trans 4:29–33
22. Gezowich DM, Geil PH (1968) Polym Engn Sci 8:202–208
23. Bodor G, Grell M, Kallo A (1964) Faserforsch Textil Tech 15:527–532
24. Farrow G (1965) J Appl Polym Sci 9:1227–1232
25. Garton A, Carlsson DJ, Sturgeon PZ, Wiles DM (1977) J Polym Sci: Polym Phys Ed 15:2013–2026